Supplementary Information

Global Survey of Cell Death Mechanisms Reveals Metabolic Regulation of Ferroptosis

Kenichi Shimada[1], Rachid Skouta[1,5], Anna Kaplan[1], Wan Seok Yang[1,6], Miki Hayano[2], Scott J. Dixon[1,7], Lewis M. Brown[4], Carlos A. Valenzuela[5], Adam J. Wolpaw[1,8], Brent R. Stockwell[1,3*]

[1]Department of Biological Sciences, [2]Department of Pharmacology, [3]Department of Chemistry. [4]Quantitative Proteomics Center, Columbia University, New York, NY 10027, USA. [5]Current address: Department of Biological Sciences, Department of Chemistry, Border Biomedical Research Center, the University of Texas at El Paso, El Paso, TX 79968, USA. [6]Current address: Department of Biological Sciences, St. John's University, Queens, NY 11439, USA. [7]Current address: Department of Biology, Stanford University, Stanford, CA 94305, USA. [8]Current address: Divisions of Hematology and Oncology, the Children's Hospital of Philadelphia, Philadelphia, PA 19104, USA. [*]Corresponding author.
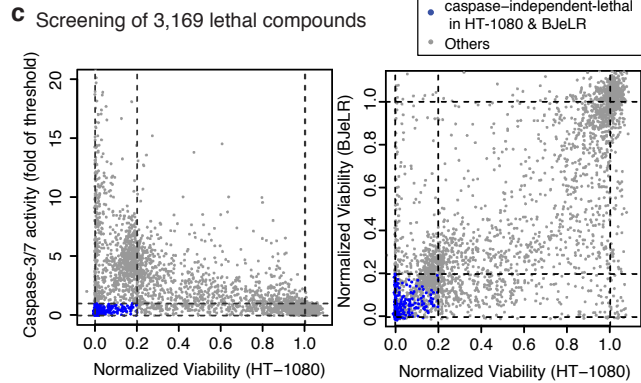
Supplementary Results
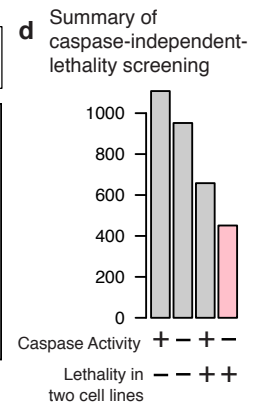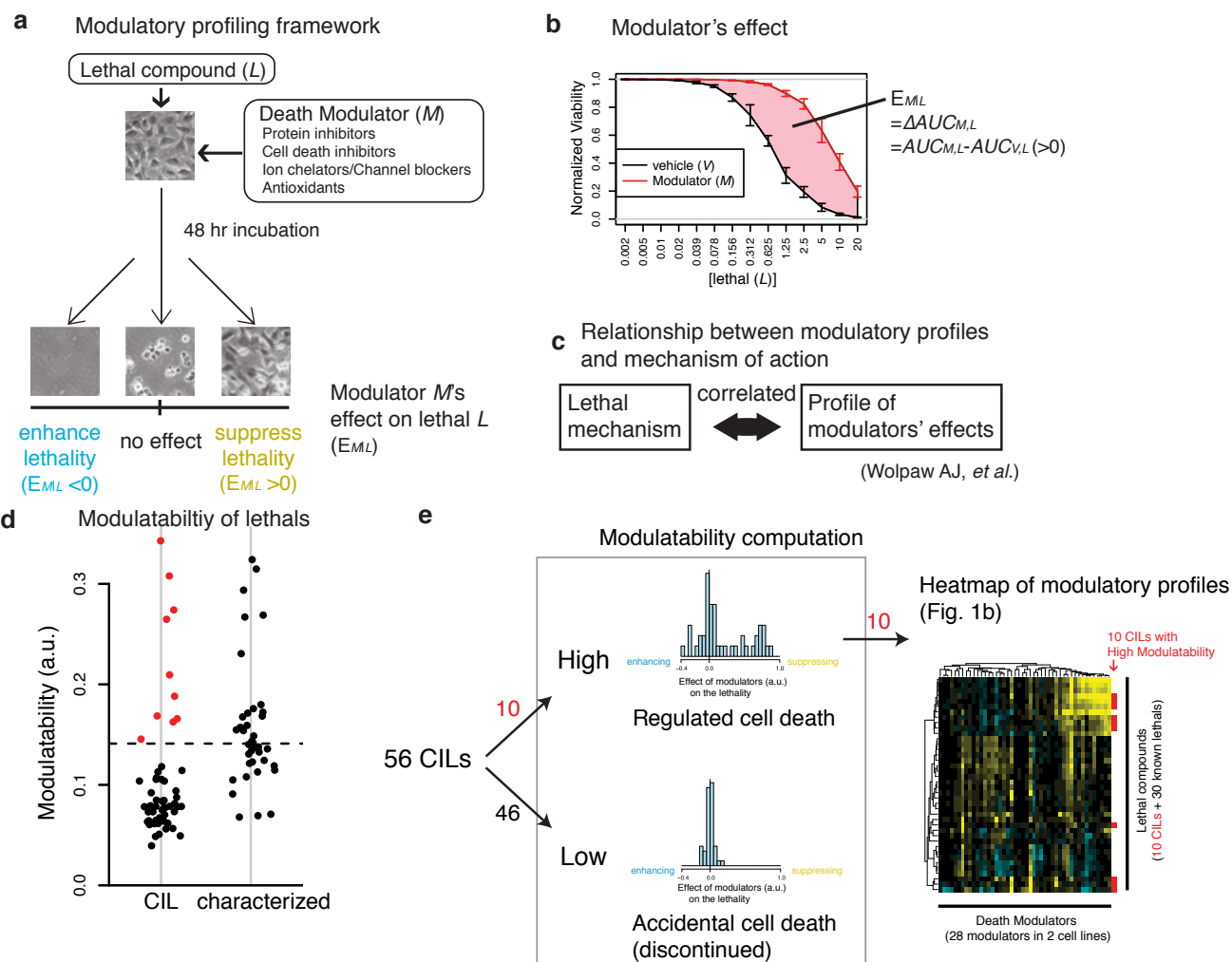
a   Caspases 3/7 activation assay
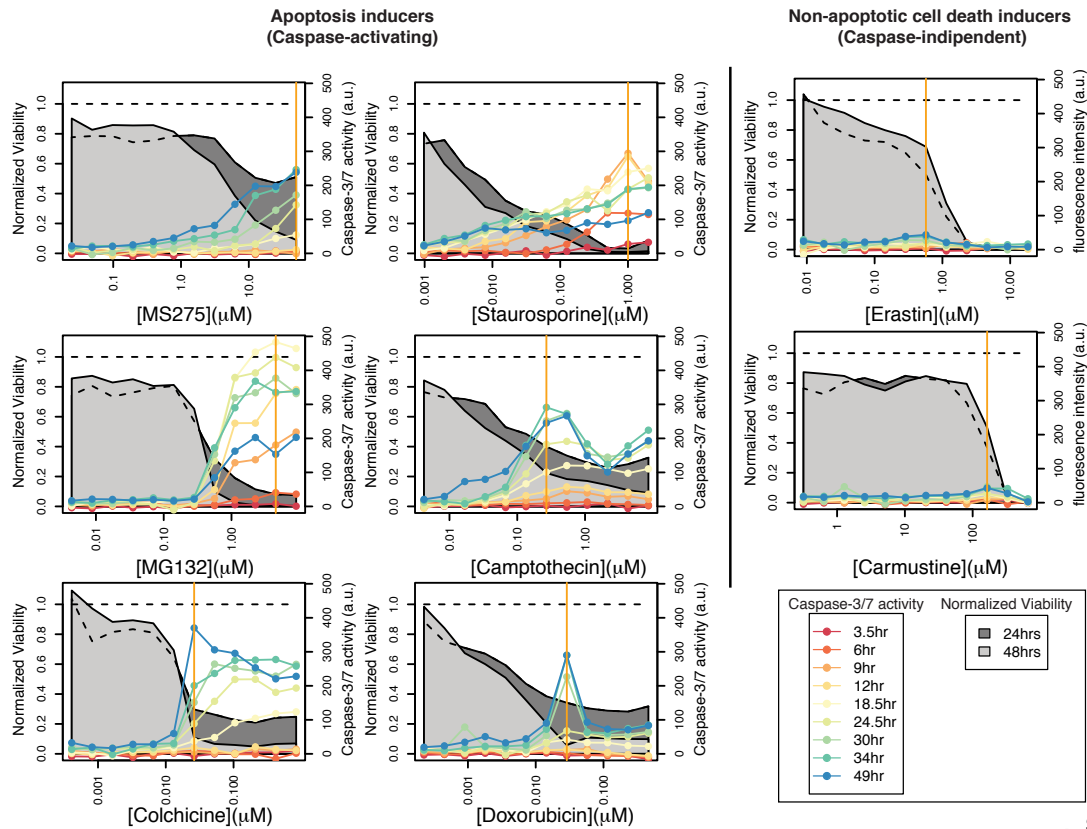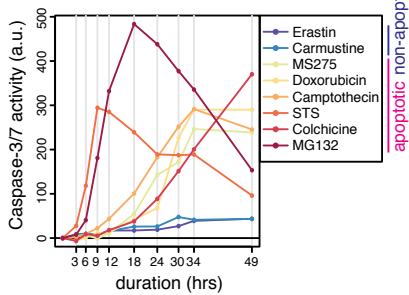
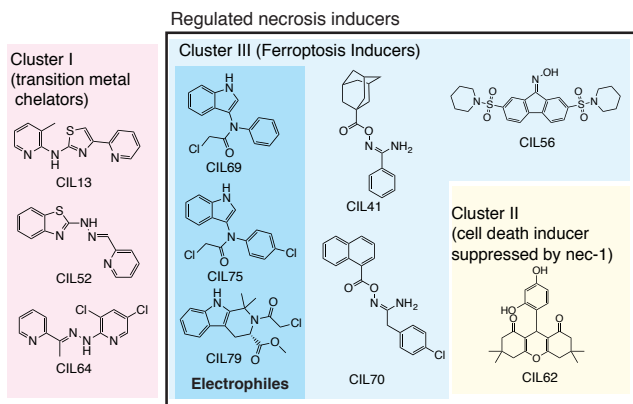**Supplementary Figure 1. Screening for caspase-3/7 independent lethal compounds (CIL)**
a. Caspase-3/7 activation assay (Apo-ONE Homogeneous caspase-3/7Assay). Six apopototic and two non-apoptotic inducers were tested to optimize the assay conditions for screening. Grey area represents normalized viability 24 or 48 hrs after lethal compound treatment, and the colored lines indicate Apo-ONE fluorescent signals after indicated time points. Vertical orange lines indicate concentrations shown in **b**. **b.** Kinetics of Apo-ONE fluorescence intensity upon lethal compound treatment. **c.** Summary of chemical screening of 3,169 compounds for caspase-independent lethality in two cell lines, HT-1080 and BJeLR cells. Blue dots represent CILs. **d.** Statistical summary of screening. The numbers of compounds lethal in both HT-1080 and BJeLR cells and/or activating caspase-3/7 are shown. Viability and Caspase-activity in **a** were tested in duplicates; representative results were shown. Screening in **c** was performed once. Plots **b** and **d** were generated from **a** and **c**, respectively.
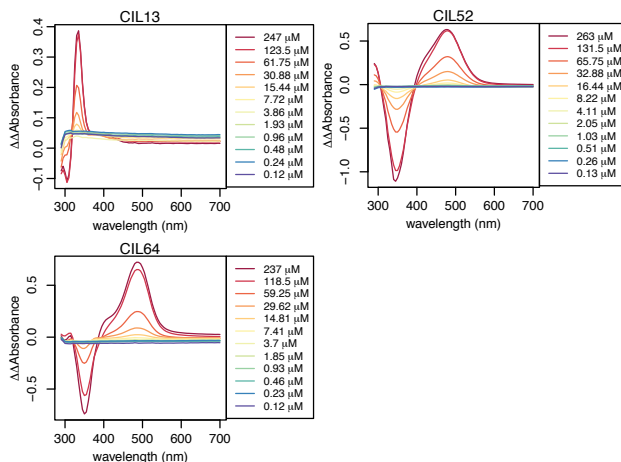
a Modulatory profiling framework

Lethal compound (*L*)

Death Modulator (*M*)
Protein inhibitors
Cell death inhibitors
Ion chelators/Channel blockers
Antioxidants

48 hr incubation

enhance lethality ($E_{ML} < 0$) no effect suppress lethality ($E_{ML} > 0$)

Modulator *M*'s effect on lethal *L* (E_{ML})

b Modulator's effect

Normalized Viability

— vehicle (*V*)
— Modulator (*M*)

[lethal (*L*)]

E_{ML}
$= \Delta AUC_{M,L}$
$= AUC_{M,L} - AUC_{V,L}$ (>0)

c Relationship between modulatory profiles and mechanism of action

Lethal mechanism — correlated — Profile of modulators' effects

(Wolpaw AJ, *et al.*)

d Modulatability of lethals

Modulatability (a.u.)

CIL   characterized

e Modulatability computation

56 CILs

High — 10 — enhancing / suppressing — Effect of modulators (a.u.) on the lethality — Regulated cell death

Low — 46 — enhancing / suppressing — Effect of modulators (a.u.) on the lethality — Accidental cell death (discontinued)

Heatmap of modulatory profiles (Fig. 1b)

10 CILs with High Modulatability

Lethal compounds (10 CILs + 30 known lethals)

Death Modulators (28 modulators in 2 cell lines)

Supplementary Figure 2. Modulatory profiling scheme and modulatability
a. Scheme of the modulatory profiling experiment. Two cell lines (HT-1080 and BJeLR) were co-treated with a lethal compound and a death modulator. **b.** The modulator (*M*)'s effect ($E_{M|L}$) on the lethal compound (*L*) was assessed by computing a difference of areas under two dose-response curves ($E_{M|L} = AUC_{modulator} - AUC_{vehicle}$). **c.** In Wolpaw *et al.*[4], modulatory profiles of lethals were correlated with their mechanisms of actions. **d.** Modulatability of 56 CILs and 30 characterized compounds. The dashed line represents the median value of the modulatability of characterized compounds. Ten CILs above the line (red dots) were defined as CILs with high modulatability, which were expected to activate specific pathway(s) to induce cell death. **e.** Scheme describing how modulatability of lethal compounds are associated with specific regulated cell-death. Plot **d** was generated from the modulatory profiles (**Fig. 1b**) and done once.
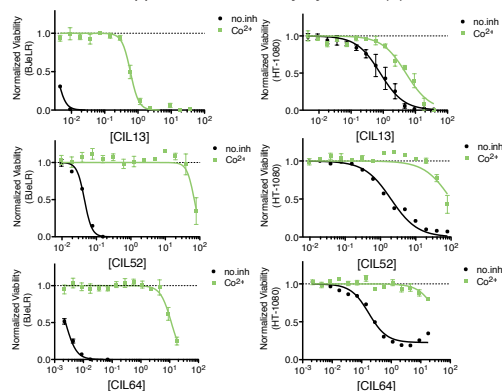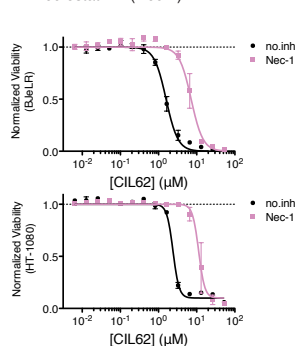
**Supplementary Figure 3. CILs with high modulatability were functionally clustered into three classes.**
a. Chemical structures of the ten CILs with high modulatability. The background colors of the compounds correspond to the clusters in Figure 1b. **b.** Changes in absorbance spectrum of each compound upon cobalt (II) supplementation *in vitro*. **c.** Suppression of CIL13, 52 and 64 with the supplementation of CoCl$_2$. **d.** 19 μM (5 μg/mL) Necrostatin-1 (Nec-1) suppressed CIL62. **e.** Both CIL62 (red) and ferroptosis inducers (orange) were suppressed by 19 μM Nec-1, but CIL62 was not suppressed by the ferroptosis inducers (antioxidants or iron-chelators). Measurements in **b** was done once; experiments in **c–e** were extracted from the modulatory profiles (**Fig. 1b**). Error bars in **c** and **d** are s.e.m. of technical triplicates.
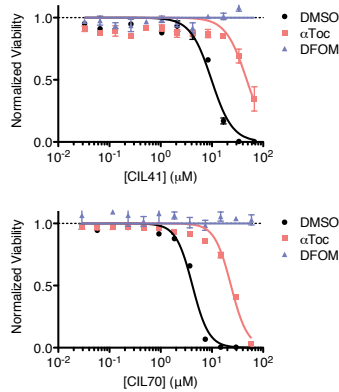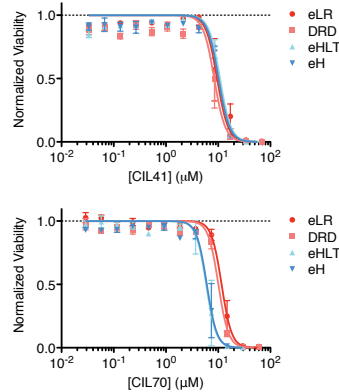
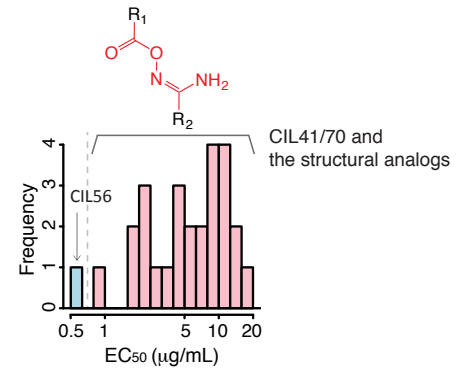**a** Classification of ferroptosis inducing-CILs.
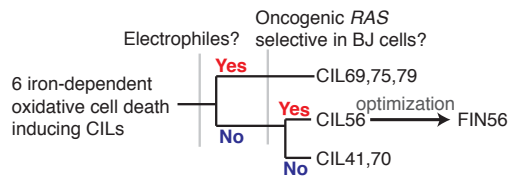
b CIL41/70 inducing ROS
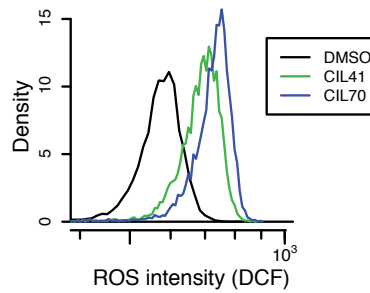
c CIL41/70 suppressed by an iron-chelator and an antioxidant.

d CIL41/70 not $HRAS^{V12}$ selective in the BJ cell series

e EC$_{50}$ of CIL56, CIL41/70 and the structural analogs of CIL41/70

Supplementary Figure 4. CIL41/70 induce iron-dependent oxidative stress but not oncogenic-*RAS* selective in the BJ series
a. Properties of 6 CILs (41, 56, 69, 70, 75, 79). **b.** CIL41/70 treatment caused H_2-DCFDA-detectable ROS generation. **c.** Suppression of CIL41/70 lethality by ferroptosis inhibitors (the antioxidant α-tocopherol (αToc) and the iron-chelator deferoxamine (DFOM)). **d.** CIL41/70 do not induce selective lethality in the BJ cell line panel. **e.** EC$_{50}$ of CIL56, CIL41/70 and the structural analogs of CIL41/70. Experiments in **b–d** were done in biological triplicates and single representative results are shown; error-bars indicate s.e.m. of technical triplicates; screening in **e** was done once.
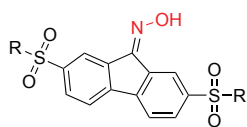
Name	R	EC$_{50}$	Selectivity (fold)
SRS5-05		0.44	2.6
SRS5-19		0.21	1.7
SRS6-27		>20	n.a.
SRS6-25		0.50	6.0
SRS6-15		8.2	2.0
SRS5-57		0.68	3.7

Name	R	EC$_{50}$	Selectivity (fold)
SRS6-23		>20	n.a.
SRS6-13		>20	n.a.
SRS8-18		>20	n.a.
SRS7-34 (FIN56)		0.24	>160
SRS8-18		>20	n.a.
SRS5-55		1.4	2.2
SRS6-51		>20	n.a.
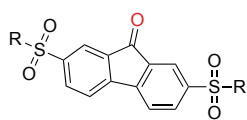
Name	R	EC$_{50}$	Selectivity (fold)
SRS1-63		>20	n.a.
SRS7-25		>20	n.a.

Supplementary Figure 5. Structure activity relationship study of CIL56 and selective induction of ferroptosis
Structural analogs of CIL56 and their capability of inducing ferroptosis. Piperidine rings and oxime group in CIL56 were substituted by different moieties. EC$_{50}$ and selectivity (fold suppression by α-tocopherol) of the synthesized analogs were shown. EC$_{50}$ and selectivity measurements were done in two biological replicates, three technical replicates each.
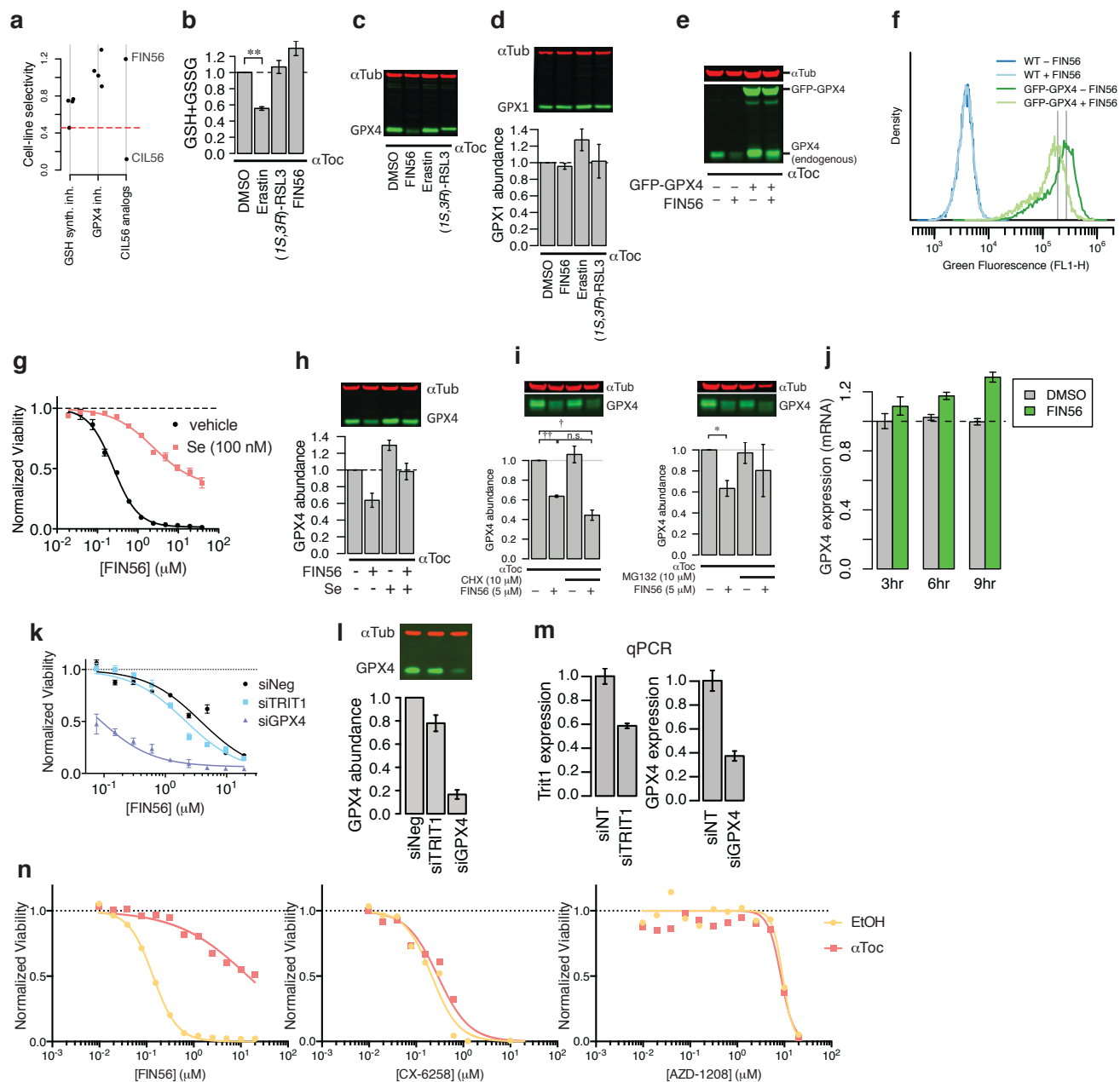
Supplementary Figure 6. Mechanisms regulating GPX4 protein abundance

a. Cell-line-selectivity of GSH synthesis inhibitors, GPX4 inhibitors, and CIL56 analogs in the NCI60 cell line panel. **b.** Abundance of total glutathione (GSH and GSSG) in HT-1080 cells upon co-treatment with 100 μM αToc and ferroptosis inducers for ten hours. αToc: α-tocopherol. **c.** GPX4 abundannce in BJeLR cells upon 100 μM αToc and ferroptosis inducers. (Corresponding western to **Figure 3c**.) **d.** GPX1 proteins in BJeLR cells upon co-treatment with 100 μM αToc and ferroptosis inducers for ten hours. GPX protein levels are normalized to α-tubulin protein levels within each sample. **e,f.** The effects of GFP-GPX4 fusion protein overexpression on endogenous and exogenous GPX4 protein abundance with or without FIN56 treatment measured using (**e**) western (corresponding to **Figure 3f**), and (**f**) FACS (green fluorescence). **g,h.** With or without pre-treatment of 100 nM selenium for 12 hrs and their effects on (**g**) FIN56 lethality in HT-1080 cells and (**h**) GPX4 abundance. **i.** The effects of translation inhibition (CHX) and proteosomal inhibition (MG132) on GPX4 abundance. **j.** GPX4 transcripts level upon 5 μM FIN56. **k.** Effects of siRNA against *GPX4* and *TRIT1* on FIN56 lethality. **l.** Effects of *GPX4* and *TRIT1* knockdown on GPX4 protein level. **m.** Efficiency of knockdown assessed by RT-qPCR. **n.** Pan-PIM inhibitors, CX-6258 and AZD-1208 were tested in 2-fold dilution series. Although they induce lethality in HT-1080 cells at higher concentrations, the lethality was not suppressed by αToc, indicating the death phenotype was not the same as ferroptosis. In **c, d, e, h,** and **i**, HT-1080 cells were co-treated with FIN56 and αToc. Experiments in **b-n** were done in biological triplicates; single representative results are shown and error-bars indicate s.e.m. of technical triplicates for **f,g,j,k,m** and **n**; mean and s.e.m. of biological triplicates were shown for **b,c,d,e,h,i** and **l**. Full gel images are in Supplementary Figure 14.
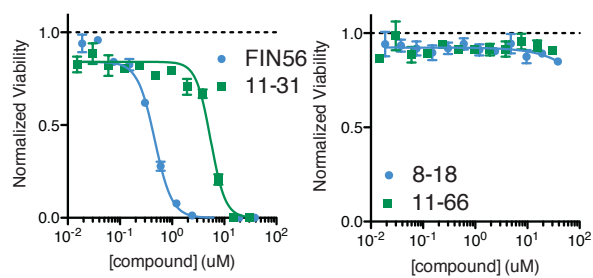
Supplementary Figure 7. Potency of CIL56 analogs in HT-1080

Potency of CIL56 analogs (Fig. **4a**) in HT-1080 cells in 48 hrs. The experiment was done in biological triplicates. Error-bars indicate s.e.m. of technical triplicates.
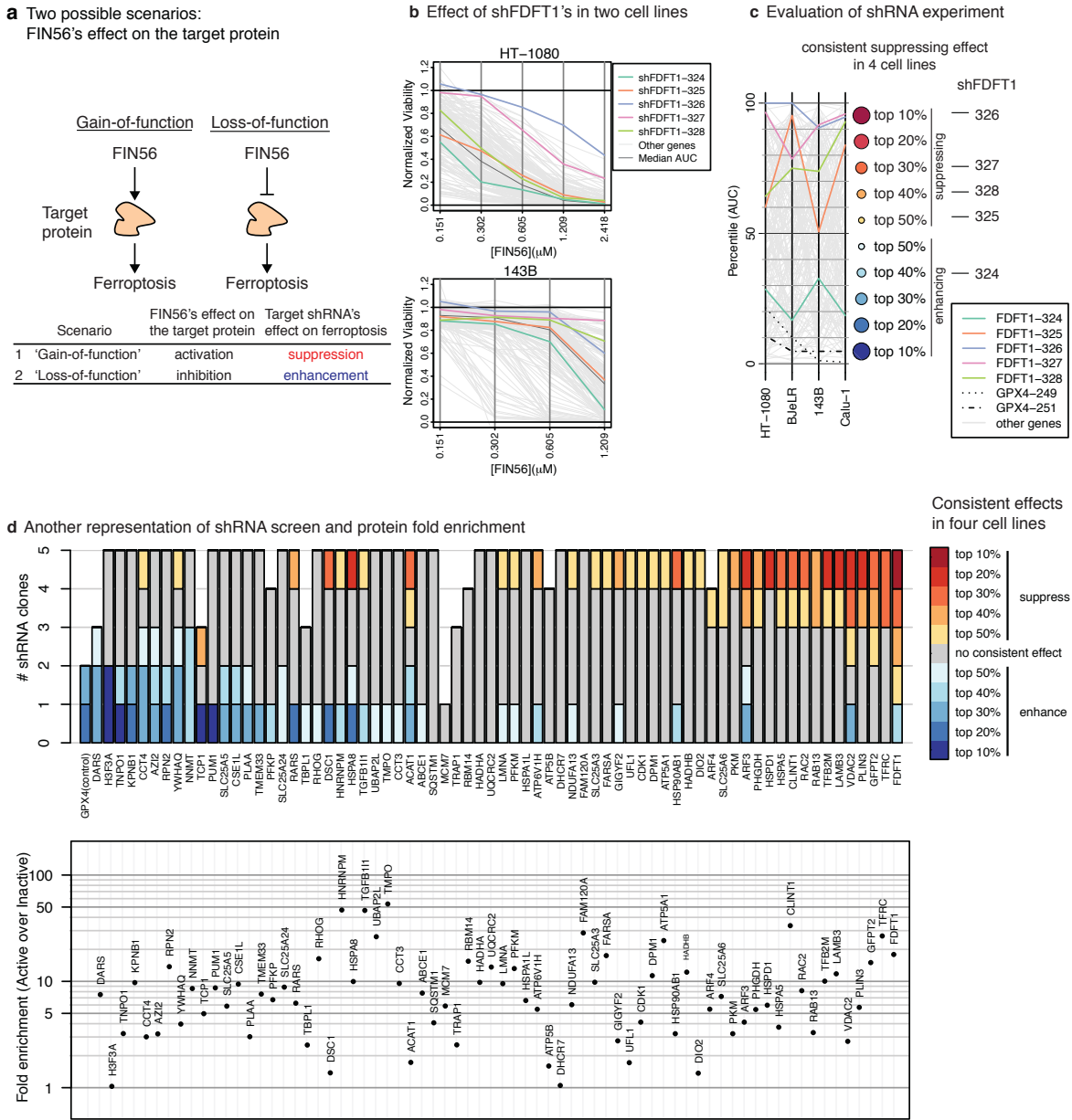
Supplementary Figure 8. Interpretation of shRNA screen experiment targeting proteins identified in chemoproteomics
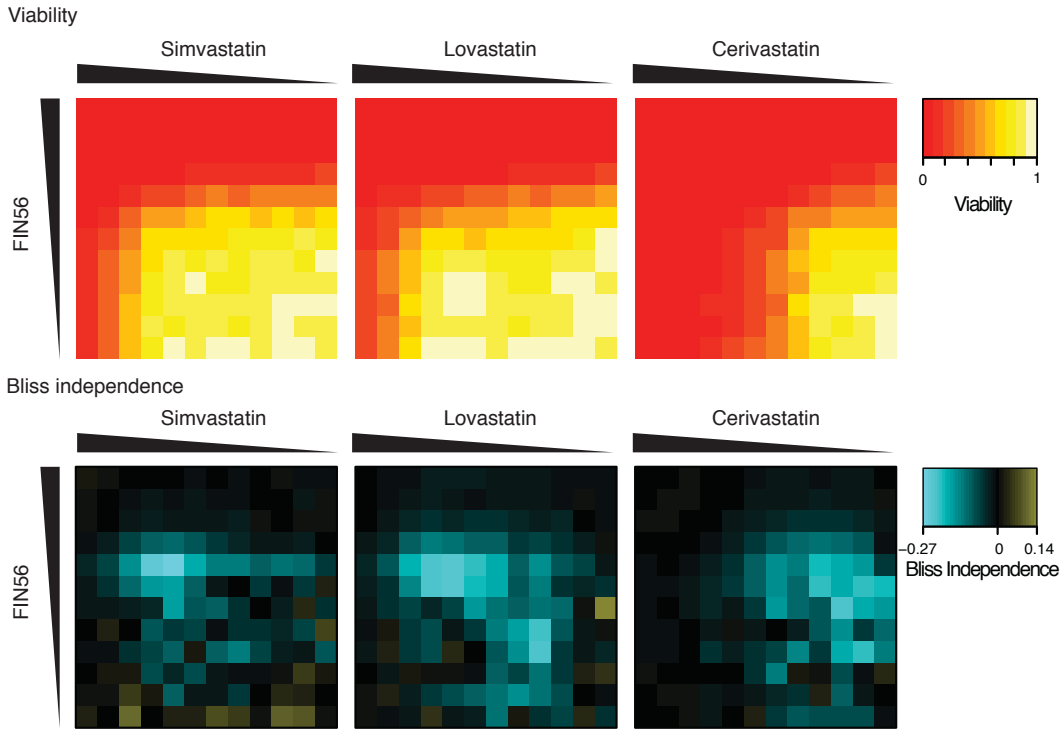**a.** Two possible scenarios when FIN56 binds to its target protein. Depending on the scenarios, expected effect of shRNAs against genuine targets on FIN56's lethality is opposite. **b.** Effects of shRNAs targeting 70 different proteins identified in chemoproteomics on FIN56. Two of the four cell lines are shown (See Fig. 4c for the other two). shFDFT1's were featured with polychromatic lines. **c.** Summary of the shRNA screens. Effects of shRNAs targeting the 70 proteins in the four cell lines. Each shRNA's effect in each cell line was represented by AUC, and ranked across the shRNAs in each cell line, The ranks were scaled between 0 and 100. Five shFDFT1 as well as two control shGPX4 are featured; shFDFT1 clones 326, 327, 328, and 325 are constantly within top 10, 20, 30, and 50 percentiles across the four cell lines. **d.** Relationship between the shRNA screen and the protein fold enrichment from the proteomic analysis. Top panel: the shRNA screen (different representation of **c.**). The height of the barplot corresponds to the number of shRNAs targeting the gene. Colors of the segments indicate each shRNA's consistent effect (red – suppression, blue – enhancement, grey – not consistent). Bottom panel: fold enrichment of protein pull-down with active probe vs inactive ones in chemoproteomic analysis. Two plots in Figure **4b** show the same result as **c,** emphasizing the ratio between '# consistent enhancer or suppressor shRNAs' vs '# shRNAs targeting each gene'. shRNA treatment and FIN56 treatment was done once in each cell line.
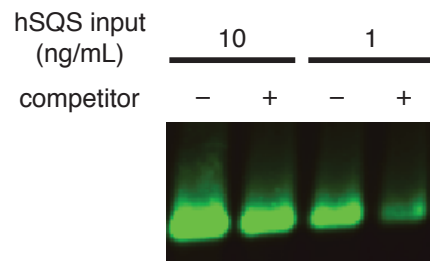
Supplementary Figure 9. SQS pulldown and competition assay
SQS pull-down using purified truncated SQS, active probe and FIN56 as competitor. 190 μL of 10 ng/mL and 1 ng/mL purified truncated human SQS were preincubated with vehicle (DMSO) or 100 μM FIN56 for two hours, and further incubated with 5 μL of active probe for another two hours. Pull-down and western were done in biological triplicates and a representative result is shown. Full gel image is in Supplementary Figure 14.

a Synergistic effect of statins vs FIN56

Viability

Simvastatin Lovastatin Cerivastatin

FIN56

Viability
0   1

Bliss independence

Simvastatin Lovastatin Cerivastatin

FIN56

−0.27   0   0.14
Bliss Independence

b statins' lethality and specificity

Normalized Viability — [Simvastatin] (μM), [Lovastatin] (μM), [Cerivastatin] (μM)

— DMSO
— mevalonolactone
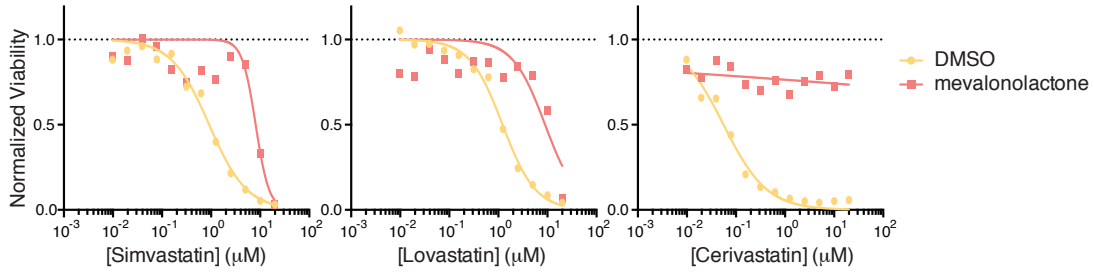
c Effects of cerivastatin/MVA on FIN56

Normalized Viability — [FIN56] (μM)

● DMSO
■ Cerivastatin
▲ MVA
▼ MVA+Cerivastatin

d Chemical perturbation of lipid synthesis and GPX4 abundance

αTub
GPX4

GPX4 expression — DMSO, Ceriv, MVA+DMSO, MVA+Ceriv
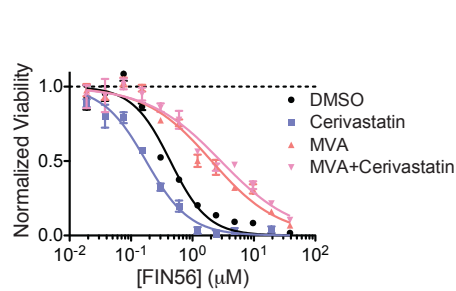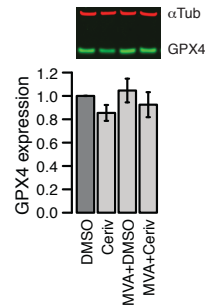
Supplementary Figure 10. Synergy between statins and FIN56
a. Synergy between three statins and FIN56 was measured and computed using Bliss independence. **b.** Three statins were tested in dilution series in HT-1080 cells with or without mevalonolactone. Lethality of Simvastatin and Lovastatin was not suppressed by mevalonolactone, indicating that they interact with off-targets at higher concentrations while cerivastatin more selectively targets HMG-CoA reductase. **c.** Effects of 1 μM cerivastatin and/or 100 μM mevalonolactone (MVA) in HT-1080 cells. **d.** Effects of supplementing the mevalonate pathway modulators for 24 hrs on GPX4 protein level in HT-1080 cells. Experiments in **a**, **c** and **d** was done in biological triplicates; **b** was done in biological duplicate; **a** and **c** show single representative results; mean of the technical triplicates were shown for viability and Bliss computation in **b**; error bars are s.e.m. in **c**; mean and s.e.m. of the biological replicates were shown in **d**. Full gel of **d** is in Supplementary Figure 14.

a. oxidative phosphorylation was not affected.
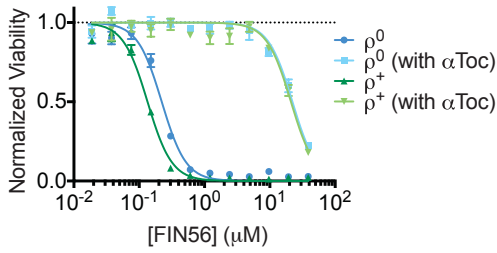
b. mitochondria-encoded genes are not expressed.
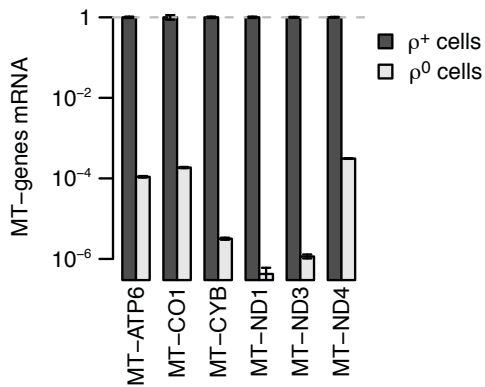
c. Lipid ROS
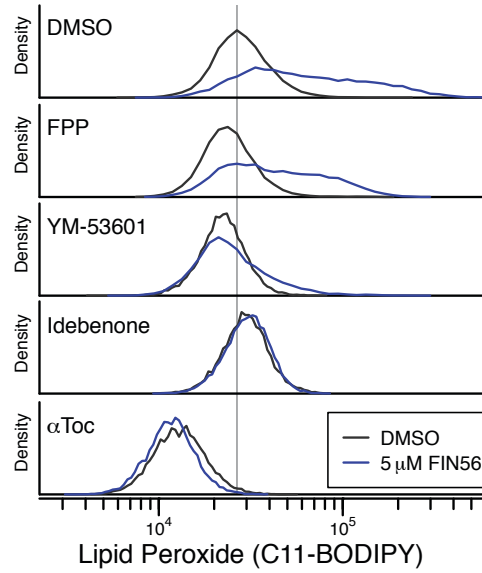
Supplementary Figure 11. Modulators of the mevalonate pathway do not target respiration chain nor act as lipid antioxidant
a. 143B lung adenocarcinoma cells with or without mitochondrial DNA (ρ^0 and ρ^+ cells) **b.** confirmation that mitochondrial DNA-encoded genes are not expressed. **c.** Lipid peroxide levels upon the mevalonate pathway modulator treatments and α-tocopherol. Experiments in **a** and **b** were done in biological singlicate and error bars are s.e.m. of three technical replicates; experiments in **c** was done in biological duplicate.
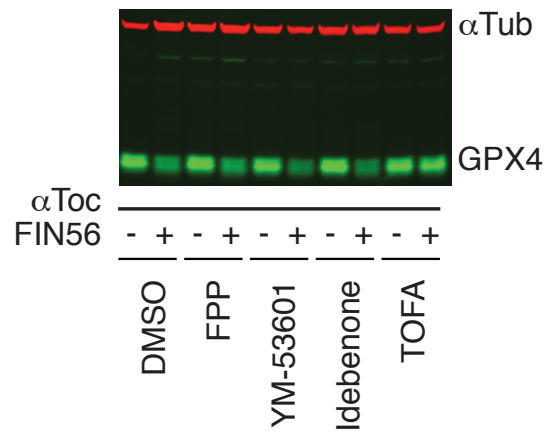
Supplementary Figure 12. Effects of the mevalonate pathway modulators and an ACC inhibitor on FIN56-induced GPX4 loss. A representative western blot of Figure 6a. Full gel image is available in Supplementary Figure 14. The western was done in three biological replicates.

a. Effect of shGPX4 on HT-1080 viability
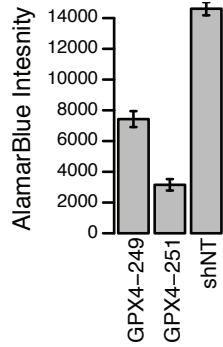
b. Effect of the mevalonat pathway modulators.
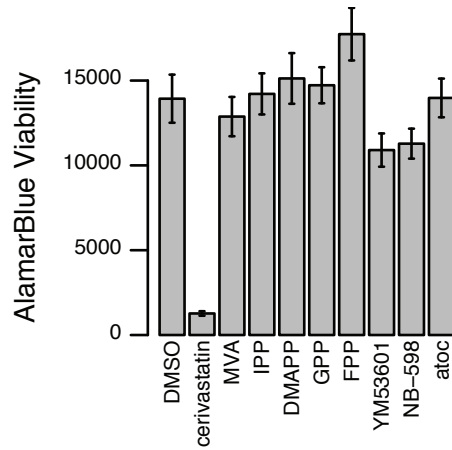
c. Effect of supplementation of metabolites derived from FPP.
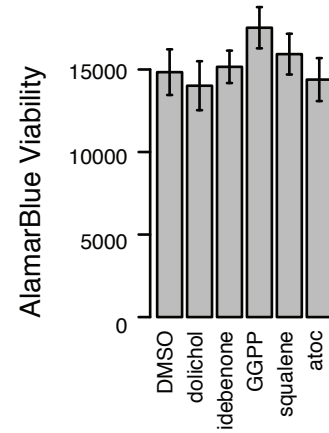
Supplementary Figure 13. Modulators' effects on HT-1080 viability.
a–c corresponds to (**a**) Figure **3c**, (**b**) Figure **5e**, and (**c**) Figure **5f**. Error bars are s.e.m. of technical triplicates.

a
GPX1 (red); actin (green)

b
GPX4 (green); actin (red)

c
GPX4 (down), GFP-GPX4(up)
(green), actin (red)

d
Se supplementation
GPX4 (green); actin (red)

e
left 4 lanes: MG132, right 4 lanes: CHX
GPX4 (green); actin (red)

f
siTRIT1 treatment
GPX4 (green); actin (red)

g
pull-down with
active vs inactive probes

h
pull-down with competition
GPX4 (green); marker (red)

i
cerivastain/MVA treatment
GPX4(green); actin (red)

j
the mevalonate pathway modulator
treatments; GPX4 (green) actin (red)

Supplementary Figure 14. Full gel images.
Corresponding figures: **a.** Suppl. Fig. 6c (left) **b.** Suppl. Fig. 6c (right) **c.** Suppl. Fig. 6d **d.** Suppl. Fig. 6g **e.** Suppl. Fig. 6h **f.** Suppl. Fig. 6k **g.** Suppl. Fig. 5c **h.** Suppl. Fig. 9 **i.** Suppl. Fig. 10d **j.** Suppl. Fig. 12.

Category	Parameter	Description
Assay	Type of assay	Cell-based assay
	Target	Casepase-independent lethality in HT-1080 and BJeLR
	Primary measurement	i) Lethality: Alamar Blue (Life Technologies) Viability in both HT-1080 and BJeLR cells. ii) Apo-ONE Homogeneous Caspase-3/7 Assay (Promega)
	Key reagents	Alamar Blue (Life Technologies); Apo-ONE Homogeneous Caspase-3/7 Assay reagents (Promega)
	Assay protocol	Grow cells treated with lethal compounds. Lysed cells and measured Apo-ONE Caspase-3/7 fluorescence after 16 hours. Separately, HT-1080 and BJeLR were incubated with compounds for 48 hours and added Alamar Blue, incubated for another 6 hours.
	Additional comments	
Library	Library size	3,169 compounds
	Library composition	Uncharacterized compounds pre-selected for lethality in BJ-eLR cell line.
	Source	Diversity-oriented library was purchased from the following companies: TimTec, InterBioScreen, ChemBridge.
	Additional comments	
Screen	Format	384 well plate
	Concentration(s) tested	5.3ug/mL
	Plate controls	DMSO (0.4%) as non-lethal control. No lethal control
	Reagent/ compound dispensing system	Beckman Coulter Biomek FX Workstation
	Detection instrument and software	Perkin Elmer Victor3
	Assay validation/QC	
	Correction factors	None
	Normalization	i) Viability: median of 28 wells with DMSO treated cells in each 384-well plate was set as one. All the wells were scaled proportionally. ii) Caspase-3/7 activity: 95 percentile of DMSO treated cells were set as one. All the wells were scaled proportionally.
	Additional comments	
Post-HTS analysis	Hit criteria	Compounds that induces i) Viability < 0.2 in both HT-1080 and BJeLR cell lines, and ii) Caspase-3/7 activity < 1 were considered caspase-independent lethal.
	Hit rate	451/3,169 = 14.2%
	Additional assay(s)	Of 451 hits, 56 structurally diverse and potent compounds were selected, purchased and tested for Modulatory Profiling.
	Confirmation of hit purity and structure	The selected 56 compounds were further reordered from another vendors, tested for caspase independent lethality in 12-point 2-fold dilution series.
	Additional comments	All 56 compounds were confirmed positive.

Supplementary Table 1. Small molecule screening data

Chemical or Genetic Modulator	Abbreviation	Mechanism	HT1080	BJeLR	conc (μM)	Ferroptosis suppressor
α-tocopherol	atoc	Antioxidant	x	x	100	x
Butylated hydroxyanisole	BHA	Antioxidant	x		140	x
Butylated hydroxytoluene	BHT	Antioxidant	x		115	x
($\pm$)-6-Hydroxy-2,5,7,8-tetramethylchromane-2-carboxylic acid	Trolox	Antioxidant	x	x	150	x
Cobalt (II)	Co2	Calcium channels blocker	x	x	1200	
Gadolinium (III)	Gd3	Calcium channels blocker (via sodium leak channel, stretch activated channel)	x	x	30	
Ethyleneglycol-O,O'-bis(2-amino ethyl) -N,N,N',N'-tetraacetic acid	EGTA	Calcium ion chelator	x		2000	
Digoxin	Dig	Inhibitor of Na$^+$/K$^+$ ATPase (increase calcium ion influx)	x		0.13	
Deferoxamine	dfom	Iron ion chelator	x		150	x
L-mimosine	Lmim	iron ion chelator, Inhibitor of cell cycle at G1-S	x	*1	175	x
Cycloheximide	CHX	Inhibitor of protein synthesis	x	x	1.5	
Actinomycin D	ActD	Inhibitor of RNA synthesis (RNAPII)	x		0.0012	
Calpain Inhibitor I	ALLN	Inhibitor of calpain I/II and cathepsins B/L	x	x	25	
Na-tosyl-lys-chloromethylketone	TLCK	Inhibitor of trypsin-like serine proteases	x	x	135	
Pepstatin	Pepstatin	Inhibitor of cathepsin D	x	x	1	
NG-Monomethyl-D-arginine	NMMA	Inhibitor of nitric oxide synthase	x	x	7	
NG-Nitro-L-arginine-methyl ester	LNAME	Inhibitor of nitric oxide synthase	x	x	300	
1,4-diamino-2,3-dicyano-1,4-bis[2-aminophenylthio] butadiene	U0126	Inhibitor of Mitogen-activated protein kinase kinase (MEK) 1/2	x		11	
Anthra(1,9-cd)pyrazol-6(2H)-one 1,9-Pyrazoloanthrone	SP600125	Inhibitor of c-Jun N-terminal kinase 1/2/3	x		10	
Cbz-val-ala-asp(OMe)-fluormethylketone	zVAD	Inhibitor of pan-caspases (apoptosis)	x	x	45	
t-butoxycarbonyl-asp-fluormethylketone	BocD	Inhibitor of pan-caspases (apoptosis)	x	x	50	
3,4-dihydro-5-[4-(1-piperidinyl)butoxy]-1(2H)-isoquinolinone	DPQ	Inhibitor of poly-ADP ribose polymerase 1(PARP1; PARP1-dependent cell death)	x	x	10	
3-methyladenine	3MA	Inhibitor of autophagosome formation (macroautophagy)	x	x	5000	
Necrostatin-1	Nec1	Inhibitor of receptor interactin protein kinase 1 (RIPK1) (necroptosis) and indoleamine 2,3-dioxygenase (IDO)	x	x	20	
Aurintricarboxylic Acid	ATA	Inhibitor of ribonuclease	x		40	
Nicotinamide adenine dinucleotide, oxidized	NAD	Activates sirtuins, endogenous electrons carrier	x	*1	2000	
β-Carotene	Bcarotene	Vitamin A precursor	x		0.2	
Cyclosporin A	CspA	Binds cyclophilin D	x		5	

*1: used both individually and as a combination (NAD+ and Lmim)

Supplementary Table 2 Death modulators used in modulatory profiling

		CIL41	CIL56	CIL69	CIL70	CIL75	CIL79
HT-1080	DMSO	5.67 (4.13 to 7.78)	0.443 (0.287 to 0.683)	0.551 (0.337 to 0.902)	4.44 (2.98 to 6.62)	0.144 (0.101 to 0.205)	0.271 (0.198 to 0.371)
iron-chelators	Deferoxamine	124 (96.3 to 159)	1.36 (0.946 to 1.94)	9.29 (6.23 to 13.9)	157 (114 to 216)	4.82 (3.75 to 6.2)	32.4 (23.7 to 44.2)
	Lmim	69.8 (65.9 to 73.8)	1.53 (1.22 to 1.94)	4.79 (3.52 to 6.52)	47.8 (34.6 to 66)	2.47 (1.67 to 3.64)	12 (9.01 to 15.9)
	atoc	50 (44 to 56.8)	2.49 (2.22 to 2.8)	6.13 (4.79 to 7.86)	32.2 (21.8 to 47.5)	2.94 (2.23 to 3.89)	11.7 (9.82 to 13.9)
antioxidants	Trolox	23.4 (20 to 27.3)	1.31 (1.08 to 1.58)	4.26 (3.45 to 5.26)	11.1 (10.2 to 12.2)	2.56 (2.22 to 2.95)	10.2 (7.42 to 14.1)
	BHA	26 (18.3 to 36.9)	2.65 (2.02 to 3.47)	4.79 (3.39 to 6.76)	13.3 (10 to 17.7)	2.75 (1.97 to 3.85)	10.1 (7.02 to 14.4)
	BHT	12.6 (9.47 to 16.7)	1.69 (1.09 to 2.61)	3.28 (2.32 to 4.62)	6.5 (4.63 to 9.12)	1.72 (1.27 to 2.34)	6.3 (4.62 to 8.58)
MEK inh	U0126	20.9 (16.6 to 26.4)	2.81 (2.2 to 3.58)	5.75 (4.01 to 8.24)	10.3 (8.06 to 13.2)	2.53 (1.72 to 3.7)	14.3 (10.7 to 19.1)
BJeLR	DMSO	3.17 (2.58 to 3.88)	0.213 (0.164 to 0.276)	0.193 (0.126 to 0.294)	1.76 (1.29 to 2.4)	0.0598 (0.0411 to 0.0868)	0.157 (0.121 to 0.204)
iron-chelators	Lmim	22.4 (14.7 to 34.1)	0.925 (0.646 to 1.32)	0.976 (0.652 to 1.46)	13.1 (9.02 to 18.9)	0.341 (0.198 to 0.589)	0.667 (0.385 to 1.16)
	Lmim_NAD	22.6 (14.7 to 34.6)	1.3 (0.884 to 1.91)	0.889 (0.698 to 1.13)	14.8 (11.7 to 18.7)	0.314 (0.209 to 0.472)	0.566 (0.469 to 0.684)
antioxidants	Trolox	23.2 (16 to 33.5)	2.03 (1.5 to 2.73)	2.05 (1.6 to 2.63)	7.1 (5.19 to 9.71)	1.1 (0.824 to 1.48)	8.32 (6.41 to 10.8)
	atoc	36.6 (27.2 to 49.3)	2.49 (1.9 to 3.26)	1.78 (1.45 to 2.2)	18.6 (15.5 to 22.3)	1.04 (0.857 to 1.26)	7.93 (6.09 to 10.3)

* unit is μM; values indicate 'mean (range within 1s.d.)'

Supplementary Table 3. EC50s of CILs classified with other ferroptosis inducers and the effects of ferroptosis suppressors on the CILs. The data are pulled out from the modulatory profiling. Values are point estimates as well as 95% confidential intervals in parentheses computed using sigmoidal curve-fitting in Prism are shown from co-treatment of modulaotrs (rows) and lethal compounds (columns) in two cell lines (HT-1080 and BJeLR). Unit: μM.